

A Novel Tunable Microstrip Patch Antenna Using Liquid Crystal

Jia-Wei Dai*, Hong-Li Peng, Yao-Ping Zhang, and Jun-Fa Mao

Abstract—This paper presents a novel tunable microstrip patch antenna using liquid crystal. It adopts a differentially-driven, aperture-coupled, and stacked-patch structure. Compared with the conventional design, this novel antenna achieves a larger frequency tuning range, much wider impedance bandwidth, higher radiation efficiency and gain. Besides, the novel antenna facilitates the bias design as the bias signal is naturally isolated from the RF signal. Both the conventional and novel antennas are designed to operate at 28 GHz using an RT/Duroid 5880 substrate and K15 liquid crystal. Results show that the novel antenna has a tuning range of 3.1%, an impedance bandwidth of 6.43%, a peak radiation efficiency of 70%, and a peak realized gain of 6.5 dBi, while the conventional antenna has the tuning range of 2.7%, impedance bandwidth of 3.57%, peak radiation efficiency of 45%, and peak realized peak gain of 4.5 dBi.

1. INTRODUCTION

Tunable antennas are desirable for modern wireless communication systems for the better use of frequency spectrum. In this context, tunable antennas have been studied intensively [1–12]. A key factor in designing tunable antennas is the technology used for realizing the tunability. The available technologies include radio frequency microelectromechanical systems (RF-MEMS) [1, 2], semiconductor solutions [3, 4] and tunable dielectrics such as ferroelectric [5, 6] and liquid crystal (LC) [7–12]. Among them, the LC technology is a promising one, because the dielectric loss of LC decreases with increasing frequency, and the manufacturing technology is mature [13].

Tunable antennas using LC are usually designed in a microstrip patch antenna structure [9–12]. The microstrip patch antenna structure has two layers of substrates and one layer of superstrate. The microstrip patch together with the microstrip feedline is printed on the bottom surface of the superstrate layer. A cavity is formed in the top substrate layer into which the LC is injected. The ground plane is printed on the top surface of the bottom substrate layer. The LC is biased with a direct current (DC) voltage applied between the patch and the ground plane. Typical LC materials are E7 and K15, developed for LC display. There has been effort taken by the material community to develop new LC for RF and microwave products. Unfortunately, they are not yet commercially available in the market or cheap enough to use for commercial applications. Hence, we focus our effort on the improvement of tunable microstrip antenna structure rather than the properties of LC. We present the design and analysis in this paper, and describe the conventional and novel tunable microstrip patch antennas using the liquid crystal in Section 2. We examine the relationship between the orientation of the LC molecules and the bias voltage in Section 3, and discuss and compare the simulated antenna performances in Section 4. Finally, we draw the conclusions in Section 5.

Received 5 December 2016, Accepted 21 January 2017, Scheduled 8 February 2017

* Corresponding author: Jia-Wei Dai (daijiawei@sjtu.edu.cn).

The authors are with the Key Laboratory for Research of Design and Electromagnetic Compatibility of High Speed, Electronic Systems, Ministry of Education, Shanghai Jiao Tong University, Shanghai 200240, China.

2. TUNABLE MICROSTRIP PATCH ANTENNA STRUCTURES

Figure 1 shows a conventional tunable microstrip patch antenna structure using the LC. It has three layers of type RT/Duroid 5880, one superstrate layer and two substrate layers. The microstrip patch fed directly with a microstrip line is etched on the bottom surface of the superstrate layer with a thickness of 0.381-mm. A cavity is formed in the central area of the top substrate layer of 0.127-mm thick. The ground plane is etched on the top surface of the bottom substrate layer of 0.127-mm thick. The cavity has a volume of $4.5 \times 6.8 \times 0.127 \text{ mm}^3$ and is fully injected with the K15 LC. It should be noted that there are two alignment layers coated on the patch and ground plane with a negligible thickness. They are used for a good pre-alignment of the LC molecules. The whole antenna structure has a size of $25 \times 25 \times 0.635 \text{ mm}^3$. To tune the antenna frequency, a DC bias voltage is directly applied between the patch and ground plane. Both bias and RF signals exist simultaneously on the microstrip line. To avoid the detrimental effect on both the DC and RF sources, a bias tee needs to be used at the input of microstrip line.

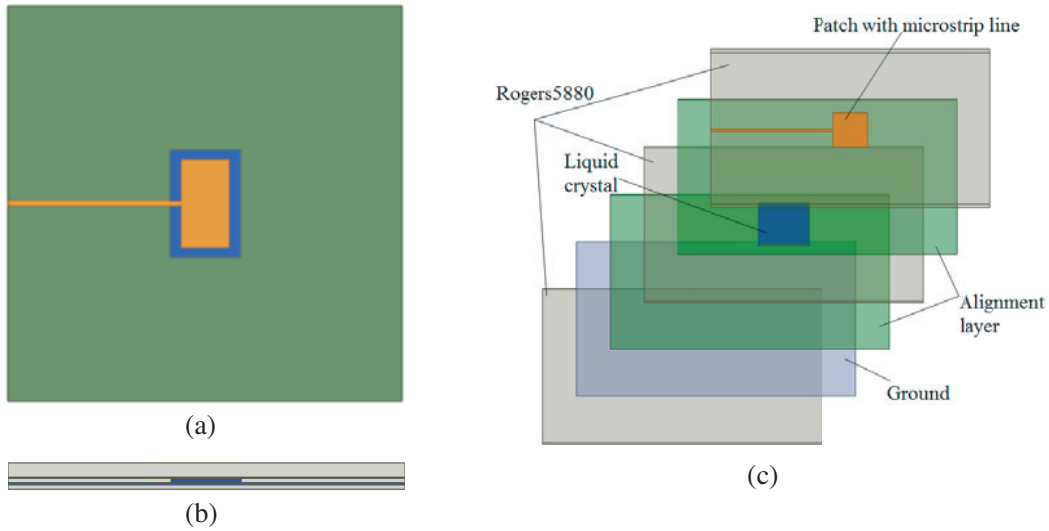


Figure 1. The conventional tunable microstrip patch antenna using the LC: (a) top view, (b) side view, and (c) perspective view.

Figure 2 shows the novel tunable microstrip patch antenna structure using the LC. Although it also has the same three layers of type RT/Duroid 5880, one superstrate layer and two substrate layers as used in the conventional design, it adopts the stacked patches, differentially driving, and aperture coupling. The stacked microstrip patches are etched, respectively, on the top and bottom surfaces of the superstrate layer with a thickness of 0.381-mm. A cavity is also formed in the central area of the top substrate layer of 0.127-mm thick. The ground plane is also etched on the top surface of the bottom substrate layer of 0.127-mm thick. To realize the differentially driving and aperture coupling, two openings are made in the ground plane, and two microstrip lines are etched on the bottom surface of the bottom substrate. The cavity has a volume of $4 \times 6 \times 0.127 \text{ mm}^3$ and is fully injected with the K15 LC. It should also be noted that there are two alignment layers coated on the patch and ground plane with a negligible thickness for a good pre-alignment of the LC molecules. The whole antenna structure has the same size of $25 \times 25 \times 0.635 \text{ mm}^3$. To tune the antenna frequency, a DC bias voltage is directly applied between the lower patch and ground plane via the DC bias pads. The two bias pads make sure the antenna structure symmetric and the DC bias voltage uniform. In this way, both DC bias and RF sources are naturally isolated. No bias tee is needed. The novel tunable microstrip patch antenna structure fully explores the advantages of the stacked patches, differentially driving and aperture coupling [14–16]. In particular, the radiation efficiency is higher when the patch width of the microstrip antenna is larger. Generally, the patch width is limited because of the undesirable influence of higher-order modes. Higher-order modes can be significantly suppressed for the differentially-driven

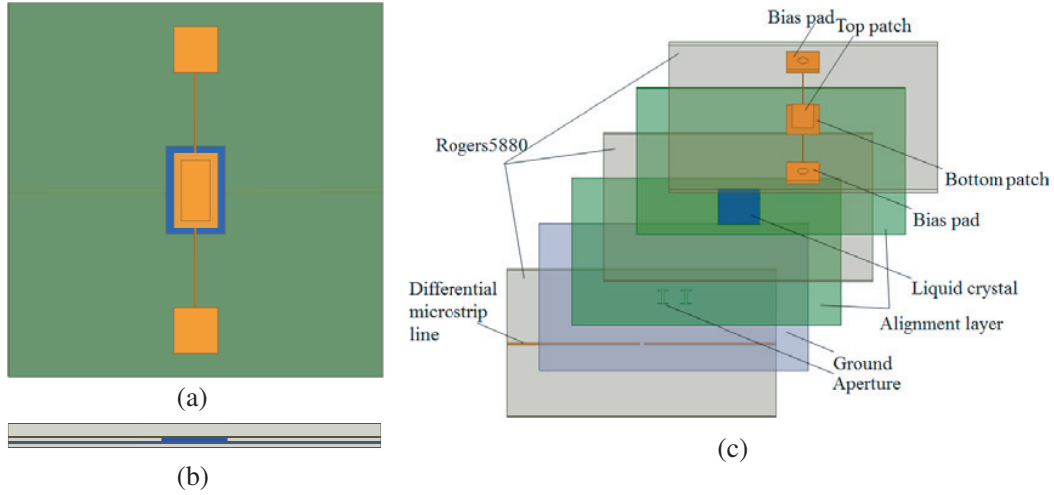


Figure 2. The novel tunable microstrip patch antenna using the LC: (a) top view, (b) side view, and (c) perspective view.

microstrip antenna, so the radiation efficiency of the differentially-driven microstrip antenna can be much higher than that of the single-ended counterpart [15], differentially driving operation is used in the novel antenna so that the radiation efficiency is higher. It is particularly suitable for highly-integrated solutions of modern wireless systems [17–19].

3. TUNABLE MECHANISM USING LIQUID CRYSTAL

The operating frequency of a microstrip patch antenna depends on the dielectric constant of its substrate. If the dielectric constant of the substrate can be changed, the operating frequency of the microstrip patch antenna can thus be tuned. The tunable mechanism of a microstrip patch antenna using the LC is illustrated in Fig. 3. As shown in Fig. 3(a), LC molecules are out of order when no alignment layer and bias voltage are applied. When alignment layers are applied as in Fig. 3(b), LC molecules tend to be ordered. They are parallel to the alignment layer, and the dielectric constant of the LC is ϵ_{\perp} . As the bias voltage is applied and increased to the maximum as in Fig. 3(c), the LC molecules tend to be inclined and parallel to the electric field between the patch and ground, and the dielectric constant of LC tends to be ϵ_{\parallel} . So the permittivity of LC can be continuously tuned from ϵ_{\perp} to ϵ_{\parallel} when a DC bias voltage is applied and increased between the patch and the ground plane as in Fig. 3(d).

The LC used is type K15. Its dielectric constant can be continuously tuned from $\epsilon_{r,\perp} = 2.72$ to $\epsilon_{r,\parallel} = 2.9$ in the 28-GHz band, and its loss tangent is about 0.03. The relationship between the orientation of the LC molecules and the bias voltage is simulated with the software DIMOS.2D to determine how much bias voltage needs to be applied. The simulated structure simplified from the antenna structures shown in Figs. 1 and 2 is shown in Fig. 4. The LC layer is 0.127-mm, the alignment layer 0.03-mm, and the metal patch and ground plane are 0.017-mm thick, respectively. By varying the bias voltage applied between the patch and ground plane, we can view from Fig. 5 the relationship between the orientation of the LC molecules and the bias voltage. Note that the green lines represent the equipotential lines.

As shown in Fig. 5, the bias voltage that causes LC molecules starting to incline is around 2–3 V, and the bias voltage that causes LC molecules stopping inclining is around 6–7 V. So if the bias voltage is smaller than 2 V, $\epsilon_r = 2.72$, and if the bias voltage is equal to or bigger than 7 V, $\epsilon_r = 2.9$, when the bias voltage is between 2 V and 7 V, ϵ_r can be approximately calculated by [20]:

$$\epsilon_r = \epsilon_{r,\perp} + \Delta\epsilon \sin^2 \varphi \quad (1)$$

where φ denotes the inclined angle of the LC molecules, and $\Delta\epsilon$ denotes the value given by [20]:

$$\Delta\epsilon = \epsilon_{r,\parallel} - \epsilon_{r,\perp} \quad (2)$$

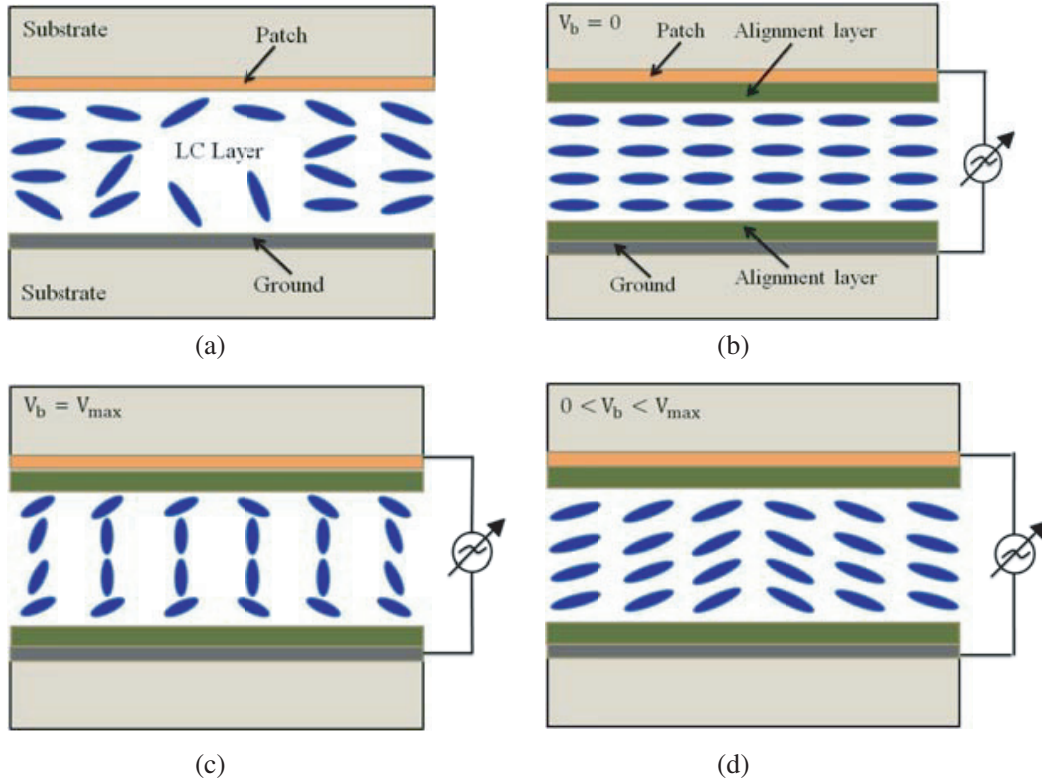


Figure 3. Illustration of tunable mechanism using the LC: (a) no alignment layer and bias voltage applied, (b) only alignment layer applied, (c) both alignment layer and maximum bias voltage applied, and (d) both alignment layer and bias voltage applied.

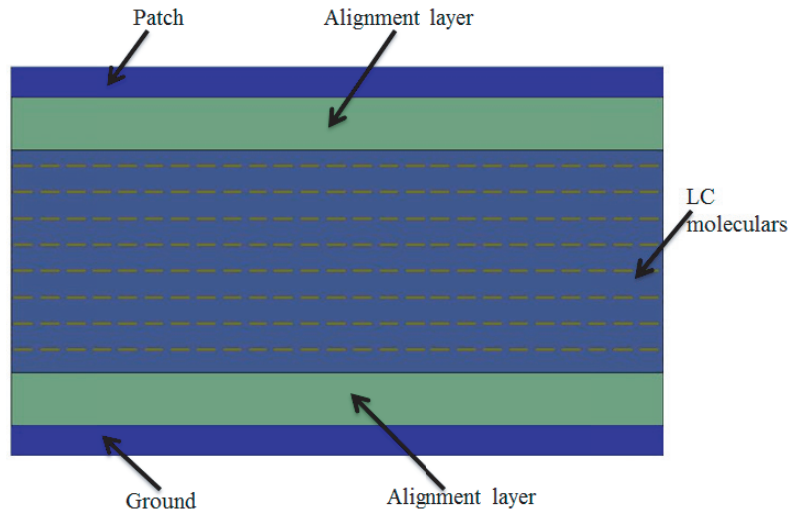


Figure 4. Simulated structure for LC molecules with a bias voltage.

4. RESULTS AND DISCUSSION

Having understood the relationship between the dielectric constant and bias voltage, one can simulate the performance of a tunable microstrip antenna by an electromagnetic solver. We use the high frequency structure simulator (HFSS) to simulate both antenna structures.

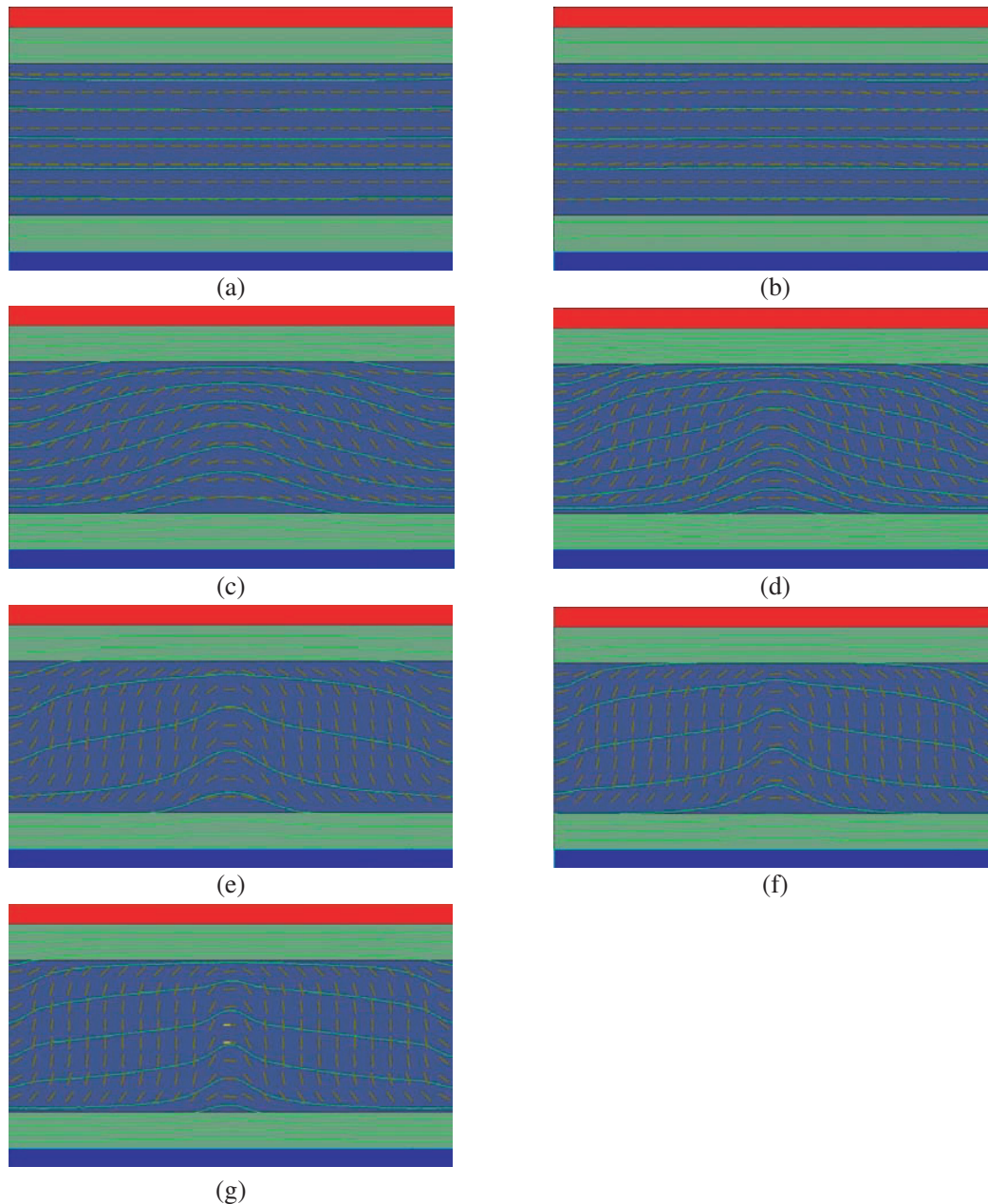


Figure 5. The orientation of LC molecules to the applied bias voltage: (a) to (g) for the bias voltage from 0 to 7 Volts.

The simulated results of the conventional tunable microstrip patch antenna are shown in Fig. 6. The microstrip patch has a size of $3.1 \times 5.6 \text{ mm}^2$. The microstrip line is designed for 50Ω . Note from Fig. 6(a) that the simulated peak matched frequency changes from 28 GHz at 0 V to 27.25 GHz at 7 V, indicating a tuning range of 2.7%. The 10-dB impedance bandwidth is about 1 GHz (or 3.57% at 28 GHz). It is evident from Figs. 6(b) and (c) that the simulated peak radiation efficiency is 45%, and the peak realized gain is 4.5 dBi at 28.25 GHz at 0 V.

The simulated results of the novel tunable microstrip patch antenna are shown in Fig. 7. The upper and lower patches have sizes of $2 \times 4 \text{ mm}^2$ and $2.7 \times 4.4 \text{ mm}^2$, respectively. The opening in the ground plane is in an H shape with the horizontal slot of $1 \times 0.1 \text{ mm}^2$ and vertical slot of $0.6 \times 0.1 \text{ mm}^2$. The separation between the two openings is 2 mm. The two microstrip lines are designed for 50Ω . Note

from Fig. 7(a) that the simulated peak matched frequency changes from 28.6 GHz at 0 V to 27.7 GHz at 7 V, indicating a tuning range of 3.1%. The 10-dB impedance bandwidth is about 1.8 GHz (or 6.43% at 28 GHz). It is evident from Figs. 7(b) and (c) that the simulated peak radiation efficiency is 70% and the peak realized gain is 6.5 dBi at 29 GHz at 0 V. The gain is very stable over the frequency range of 27–29 GHz.

Figure 8 compares the radiation patterns in E and H planes at 28 GHz. It is interesting to note that the radiation patterns of the novel antenna are more symmetrical than those of the conventional antenna. The cross-polarization radiation is much weaker for the novel antenna than the conventional one. The better radiation patterns are attributed to the differential driving and aperture coupling.

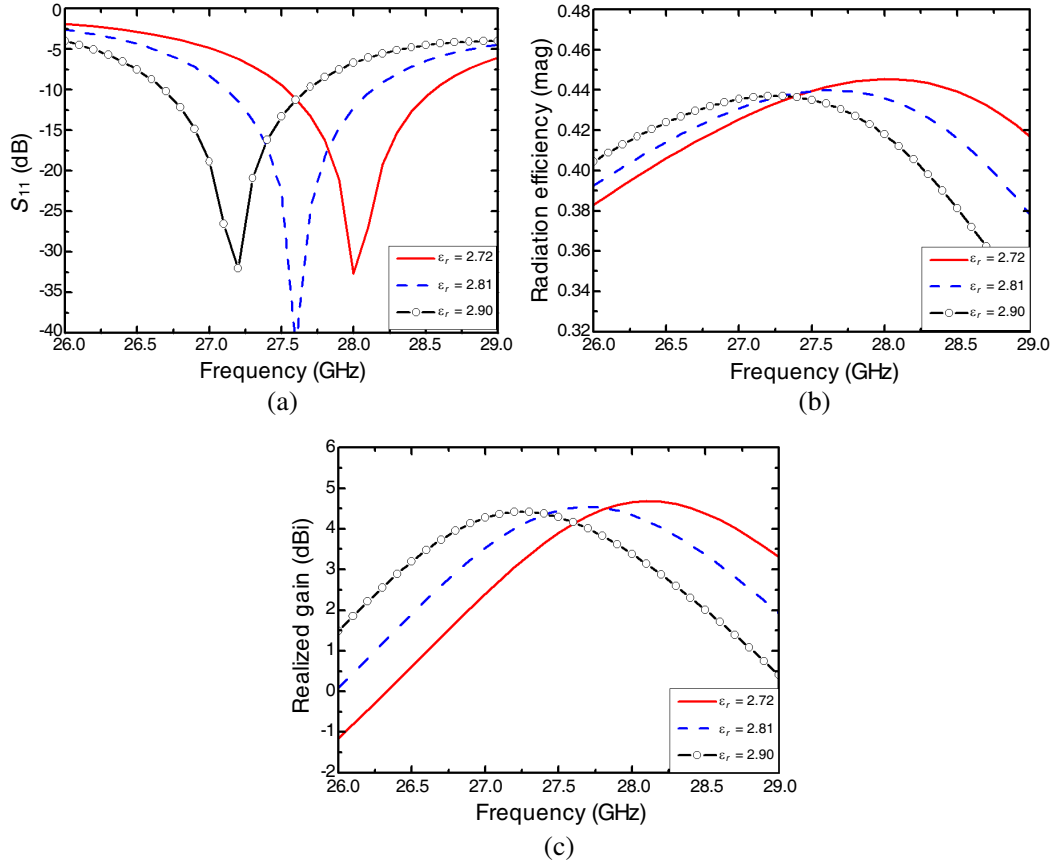
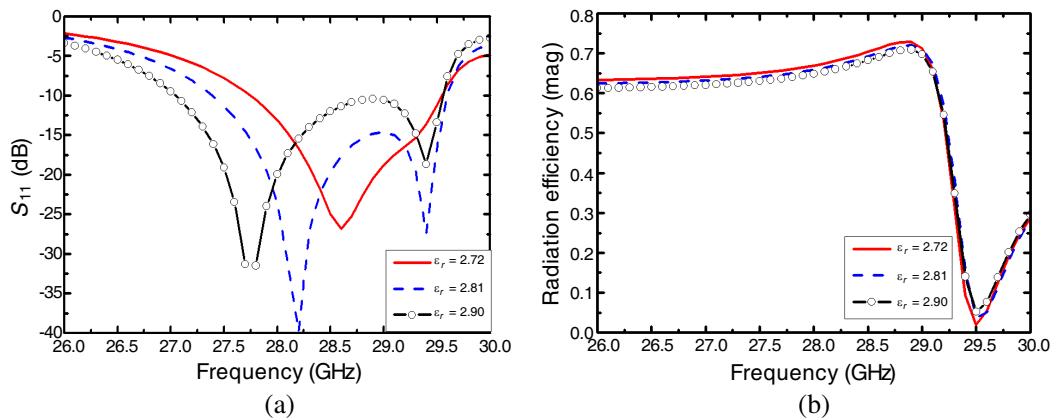


Figure 6. Simulated results for the conventional tunable microstrip patch antenna: (a) $|S_{11}|$, (b) radiation efficiency, and (c) peak realized gain.



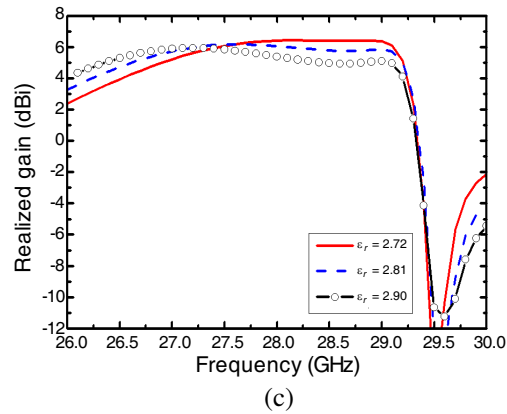


Figure 7. Simulated results for the novel tunable microstrip patch antenna: (a) $|S_{11}|$, (b) radiation efficiency, and (c) peak realized gain.

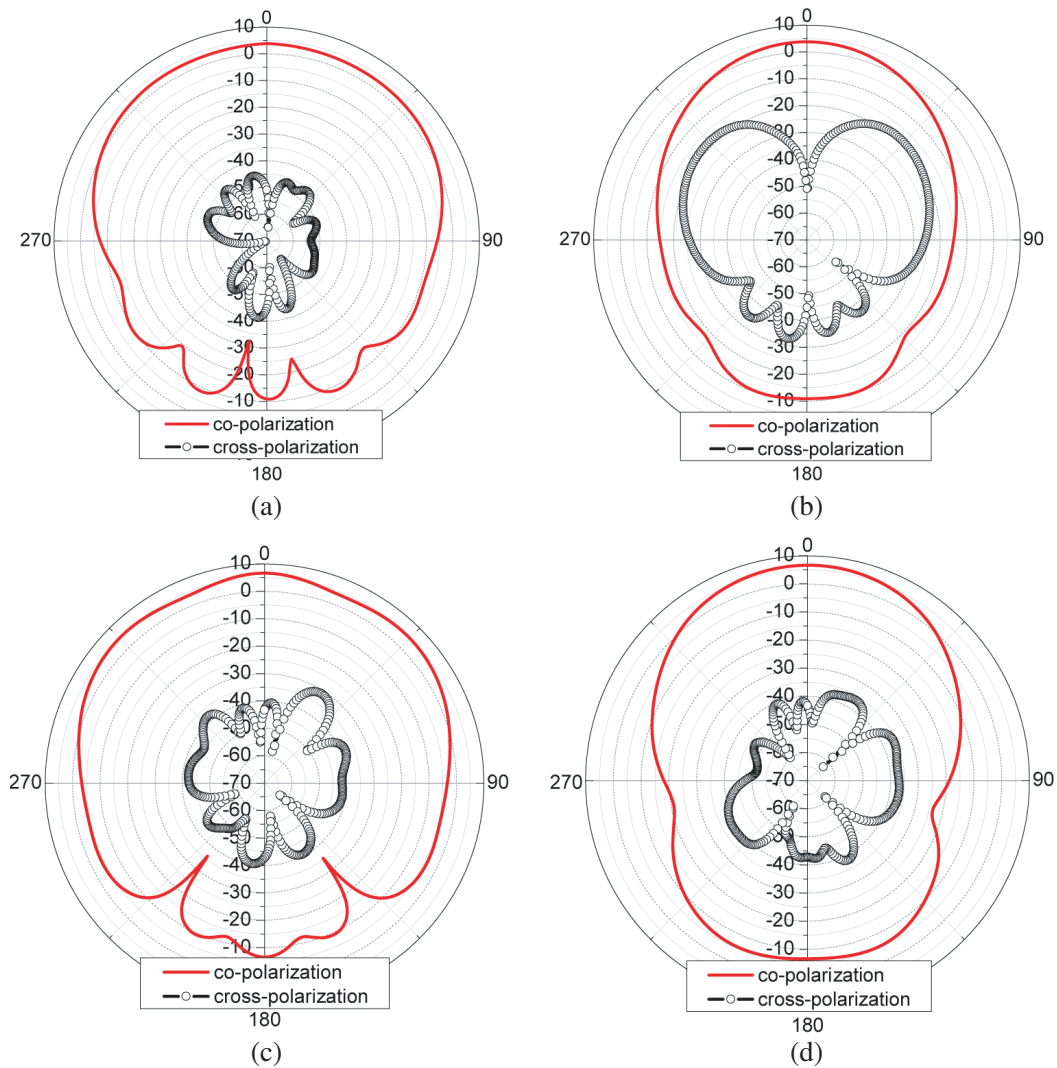


Figure 8. Simulated radiation patterns: (a) in the E and (b) the H planes for the conventional antenna, (c) in the E and (d) the H planes for the novel antenna.

The simulated key data are listed in Table 1 for the two tunable antennas.

Table 1. Comparisons between the two antennas.

| Antenna structure | Tuning range | Impedance bandwidth (GHz) | Radiation efficiency | Realized gain (dBi) |
|--------------------------|--------------|---------------------------|----------------------|---------------------|
| The conventional antenna | 2.7% | 1 (3.57%) | 45% | 4.5 |
| The novel antenna | 3.1% | 1.8 (6.43%) | 70% | 6.5 |

5. CONCLUSION

A novel tunable microstrip patch antenna using the liquid crystal is proposed for the first time in this paper. Because the differentially-driven, aperture-coupled, and stacked-patch structure is adopted, this novel antenna achieves a larger frequency tuning range, much wider impedance bandwidth, higher radiation efficiency and gain than the conventional design. Besides, the novel antenna facilitates the bias design as the bias signal is naturally isolated from the RF signal. Both the novel and conventional antennas are designed to operate at 28 GHz using an RT/Duroid 5880 substrate and K15 liquid crystal. Results show that the novel antenna has a tuning range of 3.1%, an impedance bandwidth of 6.43%, a peak radiation efficiency of 70%, and a peak realized gain of 6.5 dBi, while the conventional antenna has the tuning range of 2.7%, impedance bandwidth of 3.57%, peak radiation efficiency of 45%, and peak realized gain of 4.5 dBi.

ACKNOWLEDGMENT

This work was supported in part by the 863 Program of China under Grant No. 2015AA01A703.

REFERENCES

1. Erdil, E., K. Topalli, and M. Unlu, "Frequency tunable microstrip patch antenna using RF MEMS technology," *IEEE Trans. Antennas and Propagation*, Vol. 55, No. 4, 1193–1196, April 2007.
2. Caekenberghe, K. V. and K. Sarabandi, "A 2-bit Ka-band RF MEMS frequency tunable slot antenna," *IEEE Antennas and Wireless Propagation Letters*, Vol. 7, 179–182, March 2008.
3. Qin, P. Y., F. Wei, and Y. J. Guo, "A wideband-to-narrowband tunable antenna using a reconfigurable filter," *IEEE Trans. Antennas and Propagation*, Vol. 63, No. 5, 2282–2285, May 2015.
4. Boukarkar, A., X. Q. Lin, and Y. Jiang, "A dual-band frequency-tunable magnetic dipole antenna for WiMAX/WLAN applications," *IEEE Antennas and Wireless Propagation Letters*, Vol. 15, 492–495, July 2015.
5. Sazegar, M., Y. L. Zheng, H. Maune, C. Damm, X. H. Zhou, J. Binder, and R. Jakoby, "Low-cost phased-array antenna using compact tunable phase shifters based on ferroelectric ceramics," *IEEE Trans. Microwave Theory and Techniques*, Vol. 59, No. 5, 1265–1273, May 2011.
6. Lovat, G., P. Burghignoli, and S. Celozzi, "A tunable ferroelectric antenna for fixed-frequency scanning applications," *IEEE Antennas and Wireless Propagation Letters*, Vol. 5, No. 1, 353–356, December 2006.
7. Missaoui, S., A. Gharbi, and M. Kaddour, "Design and simulation reconfigurable liquid crystal patch antennas on foam substrate," *Journal of Chemical Engineering & Materials Science*, Vol. 2, No. 7, 96–102, 2011.
8. Palomino, G. P., M. Barba, J. A. Encinar, R. Cahill, R. Dickie, P. Baine, and M. Bain, "Design and demonstration of an electronically scanned reflectarray antenna at 100 GHz using multiresonant cells based on liquid crystals," *IEEE Trans. Antennas and Propagation*, Vol. 63, No. 8, 3722–3727, August 2015.

9. Papanicolaou, N. C., M. A. Christou, and A. C. Polycarpou, "Frequency-agile microstrip patch antenna on a biased liquid crystal substrate," *Electron. Lett.*, Vol. 51, No. 3, 202–204, February 2015.
10. Polycarpou, A. C. and M. A. Christou, "Tunable patch antenna printed on a biased nematic liquid crystal cell," *IEEE Trans. Antennas and Propagation*, Vol. 62, No. 10, 4980–4987, July 2014.
11. Liu, L. and R. J. Langley, "Liquid crystal tunable microstrip patch antenna," *Electron. Lett.*, Vol. 44, No. 20, 1179–1180, September 2008.
12. Missaoui, S., S. Missaoui, and M. Kaddour, "Reconfigurable microstrip patch antenna based on liquid crystals for microwave applications," *Proceedings of Engineering & Technology*, 23–28, 2016.
13. Deo, P., D. M. Syahkal, L. Seddon, S. E. Day, and F. A. Fernández, "Microstrip device for broadband (15–65 GHz) measurement of dielectric properties of nematic liquid crystals," *IEEE Trans. Microwave Theory and Techniques*, Vol. 63, No. 4, 1388–1398, April 2015.
14. Gao, S. C., L. W. Li, M. S. Leong, and T. S. Yeo, "A broad-band dual-polarized microstrip patch antenna with aperture coupling," *IEEE Trans. Antennas and Propagation*, Vol. 51, No. 4, 898–900, April 2003.
15. Zhang, Y. P., "Design and experiment on differentially-driven microstrip antennas," *IEEE Trans. Antennas and Propagation*, Vol. 55, No. 10, 2701–2708, October 2007.
16. Rathi, V., G. Kumar, and K. P. Ray, "Improved coupling for aperture coupled microstrip antennas," *IEEE Trans. Antennas and Propagation*, Vol. 44, No. 8, 1196–1198, August 1996.
17. Choudhary, N., A. Tiwari, J. S. Saini, V. K. Saxena, and D. Bhatnagar, "Planar arrangement of modified concentric rings with defected ground for mobile and wireless communication systems," *Progress In Electromagnetics Research B*, Vol. 47, 161–169, 2016.
18. Islam, M. T., M. N. Shakib, and N. Misran, "Broadband E-H shaped microstrip patch antenna for wireless systems," *Progress In Electromagnetics Research*, Vol. 98, 163–173, 2009.
19. Eldek, A. A., A. Z. Elsherbeni, and C. E. Smith, "Dual-wideband square slot antenna with a U-Shaped printed tuning stub for personal wireless communication systems," *Progress In Electromagnetics Research*, Vol. 53, 319–333, 2005.
20. De Gennes, P. G. and J. Prost, *The Physics of Liquid Crystals*, 2nd Edition, Clarendon Press, 1995.